10178–10189 *Nucleic Acids Research, 2017, Vol. 45, No. 17* *Published online 26 July 2017*
doi: 10.1093/nar/gkx665

Mechanism of opening a sliding clamp

Lauren G. Douma[1], Kevin K. Yu[1], Jennifer K. England[2], Marcia Levitus[2,*] and Linda B. Bloom[1,*]

[1]Department of Biochemistry & Molecular Biology and the Genetics Institute, University of Florida, Gainesville, FL 32610, USA and [2]School of Molecular Sciences and Biodesign Institute, Arizona State University, Tempe, AZ 85287, USA

Received November 04, 2016; Revised July 15, 2017; Editorial Decision July 17, 2017; Accepted July 20, 2017

ABSTRACT

Clamp loaders load ring-shaped sliding clamps onto DNA where the clamps serve as processivity factors for DNA polymerases. In the first stage of clamp loading, clamp loaders bind and stabilize clamps in an open conformation, and in the second stage, clamp loaders place the open clamps around DNA so that the clamps encircle DNA. Here, the mechanism of the initial clamp opening stage is investigated. Mutations were introduced into the *Escherichia coli* β-sliding clamp that destabilize the dimer interface to determine whether the formation of an open clamp loader–clamp complex is dependent on spontaneous clamp opening events. In other work, we showed that mutation of a positively charged Arg residue at the β-dimer interface and high NaCl concentrations destabilize the clamp, but neither facilitates the formation of an open clamp loader–clamp complex in experiments presented here. Clamp opening reactions could be fit to a minimal three-step 'bind-open-lock' model in which the clamp loader binds a closed clamp, the clamp opens, and subsequent conformational rearrangements 'lock' the clamp loader–clamp complex in a stable open conformation. Our results support a model in which the *E. coli* clamp loader actively opens the β-sliding clamp.

INTRODUCTION

Sliding clamps were first identified as components of the replisome that increase the processivity of DNA synthesis (1–4). Since their initial discovery as DNA polymerase processivity factors, sliding clamps have been found to bind directly to many different enzymes required for genome maintenance, and function both to increase enzyme residence times on DNA and to coordinate enzyme activities (reviewed in (5–7)). The ring-shaped oligomeric structure of sliding clamps is key to function by allowing sliding clamps to encircle and slide along DNA (8,9). When a DNA polymerase or another enzyme binds a sliding clamp, the enzyme is effectively anchored to the DNA template (recently reviewed in (10,11)). Most sliding clamps exist predominantly in closed ring conformations in solution and must open to be assembled on DNA by clamp loading enzymes (recently reviewed in (10,12)). Clamp loaders chaperone open clamps to DNA and release the clamps at primed template junctions where DNA synthesis will begin. Even clamps that exist predominantly as open rings, or in monomeric form, in solution are chaperoned to DNA by clamp loaders (13–15). Thus, all clamp loaders play an essential role in placing sliding clamps at the correct sites on DNA for DNA polymerases and other enzymes. Clamp loaders contain five core subunits arranged in a ring and are members of the AAA+ family of ATPases (16–18). ATP binding and hydrolysis modulate the affinity of clamp loaders for clamps and DNA to promote the assembly of clamps on DNA (14,19–24). Clamp loaders may also contain additional subunits (e.g. *Escherichia coli* ψ and χ subunits) or protein domains (e.g. the large subunit of the eukaryotic clamp loader) that mediate protein–protein and/or protein–DNA interactions at the replication fork (25–28). When bound to an open clamp, all five core clamp loader subunits interact with the surface of the clamp (29,30) (Figure 1).

Although many features of the clamp loading reaction have been defined, questions remain about the mechanism of clamp opening including how opening and closing dynamics of the clamps themselves contribute to the loading process. One possibility is that clamps spontaneously open, even if only transiently, and clamp loaders bind open clamps to stabilize the open conformation. This is the case for the bacteriophage T4 clamp that exists predominantly in an open conformation in solution (13,14). However, other sliding clamps are inherently more stable than the bacteriophage clamp, and it is not clear whether transient opening events contribute to the formation of open clamp loader–clamp complexes for these clamps. For example, the half-lives of the *E. coli* β-clamp and human PCNA-clamp on

*To whom correspondence should be addressed. Tel: +1 352 294 8379; Fax: +1 352 392 2953; Email: lbloom@ufl.edu
Correspondence may also be addressed to Marcia Levitus. Tel: +1 480 727 8586; Fax: +1 480 727 2378; Email: Marcia.Levitus@asu.edu
Present address: Jennifer K. England, Physical Sciences Inc., 20 New England Business Center Drive, Andover, MA 01810, USA.

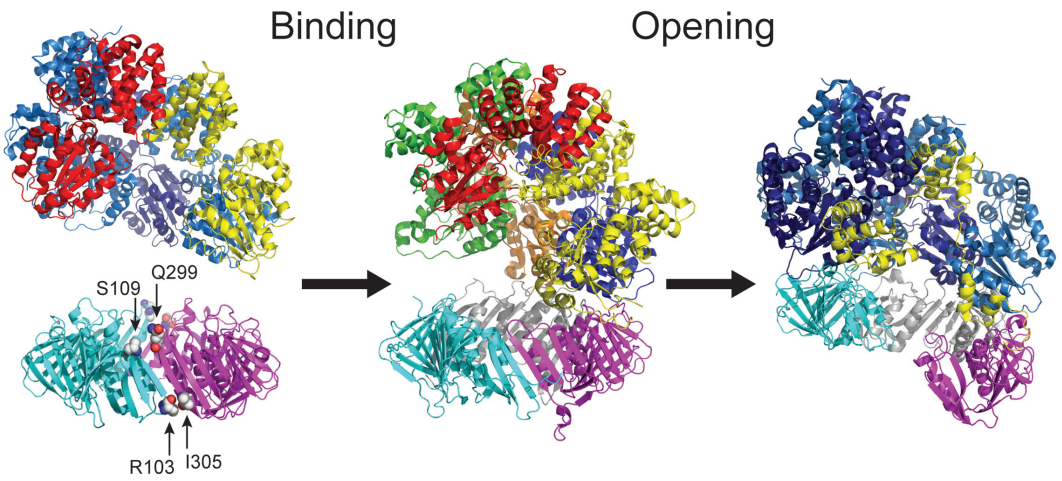

Figure 1. High-resolution structures of clamp loaders and clamps from different species depicting conformational states that may exist in the clamp opening pathway. (*Left panel*) Structures of the *E. coli* $\gamma_3\delta\delta$' clamp loader along with the β-clamp illustrate conformations that may exist prior to clamp loader–clamp binding (9,48). Amino acid residues in β that were mutated to Cys for fluorescent labeling are shown in spheres and labeled with arrows. (*Center panel*) The clamp loader initially binds the clamp to form a closed complex that may be similar in structure to the closed *S. cerevisiae* RFC–PCNA complex (44). The Rfc1 subunit (yellow) makes the most extensive interactions between the clamp loader and the clamp in the closed complex. Two of the subunits (Rfc2, green, and Rfc5, red) do not contact the surface of the clamp at all. (*Right panel*) After binding the clamp loader, the clamp either spontaneously opens or is actively opened by the clamp loader, to form an open clamp loader–clamp complex that may resemble the bacteriophage T4 gp44/62-gp45 clamp loader–clamp complex (30). In this open complex, each of the clamp loader subunits contacts the surface of the clamp such that the interaction surface is much greater than in the closed clamp loader–clamp complex.

nicked circular DNA molecules are about 72 and 24 min, respectively, at 37°C suggesting that ring-opening (or dissociation into monomers), which would allow the clamp to dissociate from DNA, is a relatively infrequent occurrence (31). But, it is possible that clamp opening dynamics are different when clamps are bound to DNA than when free in solution, or that transient opening occurs, but strong protein–DNA interactions limit dissociation. The β-dimer is exceptionally stable when free in solution with a half-life longer than 24 h at room temperature ((32) and Purohit *et al.*, *Biophysical Journal* (2017)). Although the *Saccharomyces cerevisiae* sliding clamp is not as stable, the trimer is still long lived with a half-life of ∼3 h at room temperature. Nonetheless, molecular dynamics simulations indicate that the *S. cerevisiae* RFC clamp loader simply stabilizes the open conformation of the PCNA-clamp rather than destabilizing the closed conformation suggesting that the clamp loader depends on spontaneous clamp opening to form an open clamp loader–clamp complex (33). And, studies show that backbone amide protons at the interface between protomers in the *E. coli* β-clamp exchange with deuterium suggesting that the clamp is dynamic (34). Thus, arguments can be made for and against a role for clamp loaders in actively opening sliding clamps.

This manuscript investigates the mechanism of β-clamp opening by the γ complex ($\gamma_3\delta\delta'\psi\chi$ subunits) clamp loader by determining how destabilizing the β dimer interface affects the clamp opening reaction and by defining a minimal kinetic mechanism for clamp opening.

MATERIALS AND METHODS

Buffers and reagents

Storage buffer for the β-clamp contains 20 mM Tris–HCl, pH 7.5, 0.5 mM EDTA, and 10% glycerol, and storage buffer for the γ complex (γ_{cx}) is the same except for the inclusion of 50 mM sodium chloride (NaCl), 5 mM DTT, and 30% glycerol. Stopped-flow assay buffers contain 20 mM Tris–HCl, pH 7.5, 8 mM magnesium chloride, 0.5 mM EDTA, 5 mM DTT, 4% glycerol and 50 or 500 mM sodium chloride.

Protein expression and purification

The γ form of *dnaX* along with *holA* (δ), *holB* (δ'), *holC* (χ) and *holD* (ψ) were subcloned into Duet vectors (Novagen) for expression and assembly of the γ complex (γ_{cx}) in *E. coli* BL21(DE3) cells. Cells were lysed using a French Press in 20 mM Tris–HCl, pH 7.5, 0.5 mM EDTA, 5 mM DTT, 10% glycerol and 50 mM NaCl. Affinity chromatography on a HiTrap Heparin column (GE Healthcare) was used to purify the crude supernatant followed by ion exchange chromatography on a Mono Q HR 10/10 (Pharmacia Biotech). Purified γ_{cx} was dialyzed against the storage buffer overnight and stored at –80°C. Protein concentration was determined by measuring the absorbance at 280 nm under denaturing conditions assay and using an extinction coefficient of 220 050 M^{-1} cm^{-1}. Site-directed mutagenesis of *dnaN* (β) to create mutants in Table 1 is described in (Purohit *et al.*, *Biophysical Journal* (2017)). Typical labeling efficiencies with AF488 were ≥85% per Cys residue. The stabilities of the β constructs containing the S109C/Q299C/C260S/C333S mutations needed for labeling with two fluorophores were measured by differential scanning calorimetry and compared to clamps lacking these

mutations. Overall, β clamps with the mutations for fluorescence labeling are less stable than the clamps (wild-type β and β-R103S) lacking these mutations with T_m values that are 8–10°C lower. But importantly, the R103S mutation and increased NaCl concentrations affect the stability of β-S109C/Q299C/C260S/C333S and β-wild-type clamps in the same way (Purohit *et al.*, *Biophysical Journal* (2017)).

Equilibrium clamp loader–clamp binding/opening

A QuantaMaster QM1 spectrofluorometer (Photon Technology International) was used to measure steady-state AF488 fluorescence in equilibrium binding assays. Fluorescence emission spectra were measured at each γ_{cx} concentration in an initial experiment, and all subsequent experiments were done by measuring time-based scans at a single wavelength to ensure that the system had reached equilibrium. For time-based scans, AF488 was excited at 495 nm and emission measured at 520 nm using a 3 nm bandpass. Data was collected at 1 s intervals for 2 min for assays in 50 mM NaCl and at 1 s intervals for 4 min in assays with 500 mM NaCl, and the last 30 s were averaged to obtain a value for the fluorescence intensity. Equilibrium binding was measured at a constant concentration (10 nM) of β-S109C/Q299C-$(AF488)_2$ or β-S109C/Q299C/R103S-$(AF488)_2$ and concentrations of γ_{cx} ranging from 0.1 to 1000 nM. A separate solution was made at each γ_{cx} concentration by sequentially adding to the cuvette: assay buffer (64 μL) to measure background signal, β-$(AF488)_2$ (8 μl) to measure the signal for unbound β, and γ_{cx} (8 μl) to measure the signal for complex formation. Relative AF488 intensity at each γ_{cx} concentration was calculated by dividing the fluorescence for the complex (after adding γ_{cx}) by the fluorescence of unbound β-$(AF488)_2$ (before adding γ_{cx}). An apparent dissociation constant ($K_{d,app}$) was calculated by fitting the relative intensity data (I_{obs}) to a quadratic equation using KaleidaGraph:

$$I_{obs} = \frac{(\gamma_o + \beta_o + K_{d,\,app}) - \sqrt{(\gamma_o + \beta_o + K_{d,\,app})^2 - 4\gamma_o\beta_o}}{2\beta_o}\,(I_{max} - I_{min}) + I_{min}$$

where γ_o and β_o are the total concentrations of γ_{cx} and β-$(AF488)_2$, respectively, added to the cuvette, and I_{max} and I_{min} are the limiting fluorescence intensities for bound and free β-$(AF488)_2$, respectively.

Kinetic measurements of clamp loader–clamp binding/opening, dissociation and clamp loading

Reactions were measured using a SX20MV stopped-flow fluorimeter (Applied Photophysics Ltd.). AF488 was excited at 490 nm using a 3.7 nm bandpass and emission was measured using a 515 nm cut-on filter, and steady-state AF488 fluorescence was measured on a millisecond timescale. For clamp binding/opening and clamp loading reactions, measurements were made at 1 ms intervals for 10 s, and for clamp loader–clamp dissociation, a split time-base was used in which data was collected at 1 ms intervals for the first 10 s and 50 ms intervals for the remaining time (to 500 s). Single mix experiments in which equal volumes of two solutions are mixed immediately prior to entering the cuvette were used for all kinetic assays. Clamp loader–clamp binding/opening was measured by mixing a solution containing γ_{cx} and ATP with a solution containing β and ATP. Clamp loader–clamp dissociation was measured by mixing a solution of γ_{cx}, β and ATP with a solution containing 20-fold excess unlabeled β. And, clamp loading was measured by addition of a solution containing γ_{cx}, β and ATP to a solution of DNA, SSB, and excess unlabeled clamp. Final concentrations of reagents are given for each experiment in the Figure Legends. Reaction time courses were initially fit empirically to sums of exponentials to calculate rates of reactions and determine how γ_{cx} concentration, β mutations and NaCl affect reaction rates. Time-dependent changes in intensity for clamp binding/opening reactions and for clamp loader–clamp dissociation reaction were fit to the sum of two exponentials:

$$I\,(t) = a_1 e^{-k_1 t} + a_2 e^{-k_2 t} + c$$

where k_1 and k_2 are rates and a_1 and a_2 are amplitudes of the two reaction phases and c is a constant. GraphPad Prism was used to globally fit clamp binding and opening time courses to a shared set of amplitudes and individual rate constants. KaleidaGraph was used to fit clamp dissociation time courses individually to calculate rates and amplitudes.

Kinetic modeling

Reaction time courses for clamp binding using β-S109C-AF488 and clamp opening using β-R103C/I305C-$(AF488)_2$ were globally fit to kinetic models using KinTek Explorer (35). For binding reactions, γ_{cx} concentrations ranged from 10 to 1280 nM and β-S109C-AF488 was held constant at 20 nM. For clamp opening reactions, γ_{cx} concentrations ranged from 5 to 1800 nM and β-R103C/I305C-$(AF488)_2$ was held constant at 16 nM. For the binding reactions with β-S109C-AF488, three fluorescent states were assumed, one for free/unbound clamps, one for clamp loader–clamp complexes in a closed conformation, and one for all clamp loader–clamp complexes in an open conformation. Low γ_{cx} concentration data could be fit using two fluorescent states one for unbound clamps and one for all clamp loader–clamp complexes, but at higher concentrations this two-state model did not fit the data well because the fluorescence decay of the calculated curves tended to be faster than for the data. Relative fluorescence intensities of intermediate states were fit as adjustable parameters but did not change significantly from our initial relative intensity estimates (based on exponential fits) of 1.0 for free clamps, 0.9 for the closed clamp loader–clamp complex and 0.88 for open clamp loader–clamp complexes. For the clamp opening reactions with β-R103C/I305C-$(AF488)_2$, two fluorescent states were assumed, one relative intensity associated with closed clamps and another associated with open clamps. The relative intensities were fit as adjustable parameters but did not vary significantly from our estimates, based on exponential fits of the data, of 1.0 for closed clamps and 2.8 for closed clamps.

RESULTS

Mutations to amino acid residues at the β dimer interfaces

In other work, we showed that mutations to charged residues at the β-dimer interface and high salt concentra-

Table 1. β mutants and nomenclature

β Designation	Mutations
β-S109C-AF488[a]	C260S + C333S + S109C
β-Q299C-AF488	C260S + C333S + Q299C
β-S109C/Q299C-$(AF488)_2$	C260S + C333S + S109C + Q299C
β-S109C/Q299C/R103S-$(AF488)_2$	C260S + C333S + S109C + Q299C + R103S
β-R103S/I305C-$(AF488)_2$	C260S + C333S + R103C + I305C

[a]Cys residues are labeled with Alexa Fluor 488 maleimide (AF488).

tions destabilize the β-dimer by increasing the rate of dissociation into monomers (Purohit *et al.*, *Biophysical Journal* (2017)). This work investigates the effects of destabilization of the β dimer interface on interactions with the clamp loader and steps in the clamp loading reaction. Doubly-labeled β-clamps were made by mutating Ser-109 and Gln-299 to Cys to incorporate two Alexa Fluor 488 (AF488) fluorophores in each β monomer. This doubly-labeled clamp is referred to as β-S109C/Q299C-$(AF488)_2$ (Table 1). A mutation shown to destabilize the β-dimer, Arg-103 to Ser (R103S), was incorporated into a second doubly-labeled clamp and is referred to as β-S109C/Q299C/R103S-$(AF488)_2$ (Purohit *et al.*, *Biophysical Journal* (2017)). The fluorophores are positioned at both dimer interfaces such that a pair of fluorophores, one on each monomer, interacts across the interface. When the clamp is closed the fluorophores stack and self-quench. Clamp opening separates a pair of fluorophores and increases fluorescence (32,36). Alexa Fluor 488 gives a better signal-to-noise ratio in stopped-flow clamp opening reactions than the tetramethylrhodamine (TMR) probe used in previous work ((Purohit *et al.*, *Biophysical Journal* (2017)) and Supplementary Figure S1), and for that reason was used in this study.

Effects of dimer interface destabilization on equilibrium clamp loader–clamp binding/opening

When bound to ATP, the *E. coli* clamp loader binds the β-clamp with high affinity to form an open clamp loader–clamp complex (20,37). Equilibrium clamp loader–clamp binding/opening was measured to determine whether the R103S mutation or a high salt (500 mM NaCl) concentration, both of which destabilize the β dimer interface, promote ring-opening by the clamp loader. If clamp opening by the clamp loader were dependent on clamp dynamics, then destabilization of the interface would be expected to promote opening. The *E. coli* clamp loader, γ complex (γ_{cx}), containing $\gamma_3\delta\delta'\psi\chi$ subunits, was used in this work. The increase in fluorescence that occurs when γ_{cx} binds and opens doubly-labeled clamps was measured for β-S109C/Q299C-$(AF488)_2$ and β-S109C/Q299C/R103S-$(AF488)_2$ in buffer containing 50 mM NaCl. Relative AF488 fluorescence as a function of γ_{cx} concentration is plotted in Figure 2A. Because the efficiency of protein labeling differs for different protein preparations, the magnitude of the fluorescence change differs for β-S109C/Q299C-$(AF488)_2$ and β-S109C/Q299C/R103S-$(AF488)_2$. Data were fit to the two-state binding model illustrated in the cartoon using a quadratic equation to calculate apparent dissociation constants, $K_{d,app}$, of 7.0 ± 0.4 and 4.2 ± 1.5 nM for β-S109C/Q299C-$(AF488)_2$ and β-S109C/Q299C/R103S-$(AF488)_2$, respectively. The average $K_{d,app}$ value is ∼67% larger for β-S109C/Q299C-

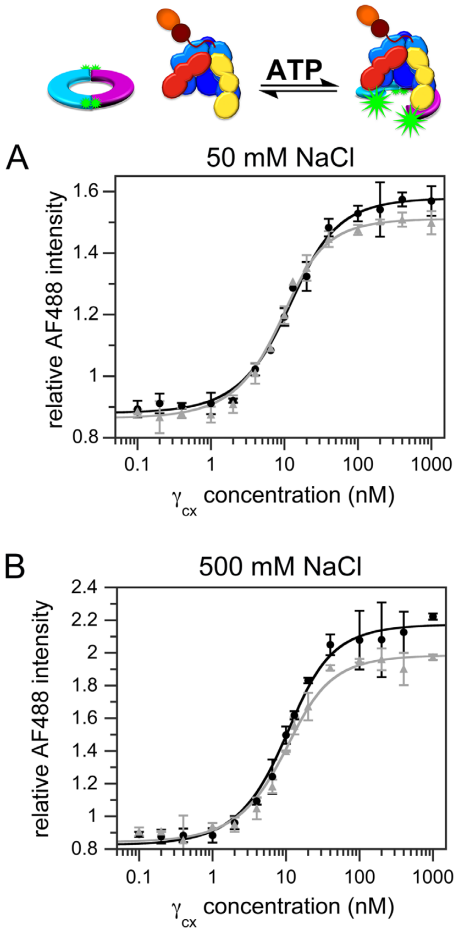

Figure 2. Equilibrium binding to form open clamp loader–clamp complexes. Relative AF488 fluorescence is plotted as a function of γ_{cx} concentration for solutions of β-S109C/Q299C-$(AF488)_2$ (black circles) and β-S109C/Q299C/R103S-$(AF488)_2$ (grey triangles) in assay buffer containing (**A**) 50 mM NaCl or (**B**) 500 mM NaCl. Final concentrations of β clamps were 10 nM. Data were fit to a quadratic equation (solid line through data points) assuming a two-state binding model (indicated in the diagram) to calculate apparent dissociation constants, $K_{d,app}$. Assay buffer contained 20 mM Tris–HCl pH 7.5, 8 mM $MgCl_2$, 5 mM DTT, 40 μg/ml BSA, 0.1 mM EDTA and 4% glycerol. Note that NaCl quenches the fluorescence of AF488 in unbound β-clamps in a concentration-dependent manner so that the magnitude of the signal change is greater in the assay containing 500 mM NaCl. Increased ionic strength likely increases the fraction of AF488 molecules that are stacked and quenched when the clamp is closed.

$(AF488)_2$ than for β-S109C/Q299C/R103S-$(AF488)_2$, and calculated $K_{d,app}$ values for β-S109C/Q299C-$(AF488)_2$ are consistently greater than for β-S109C/Q299C/R103S-$(AF488)_2$ in each of the three experiments showing that the R103S mutation modestly increases the affinity of the clamp loader for the clamp.

The titration of doubly-labeled clamps with γ_{cx} was repeated in assay buffer containing 500 mM NaCl (Figure 2B). The decrease in dimer stability for β-S109C/Q299C/R103S-$(AF488)_2$ in 500 mM NaCl was apparent in these experiments. In the absence of γ_{cx} and at low γ_{cx} concentrations where the majority of the β-clamp is not bound, the fluorescence of β-S109C/Q299C/R103S-$(AF488)_2$, but not β- S109C/Q299C-$(AF488)_2$, increased slowly over time, presumably due to dissociation of the dimer into monomers (Purohit *et al.*, *Biophysical Journal* (2017)) when diluted 10-fold into the cuvette (Supplementary Figure S2). At high concentrations of γ_{cx} where the majority of the β-clamp is bound by γ_{cx} and stabilized as open dimers, the fluorescence signal remained constant for both clamps. Due to the instability of β-S109C/Q299C/R103S-$(AF488)_2$ during the course of the titration, the $K_{d,app}$ value for the γ_{cx} and the mutant clamp cannot be rigorously determined. But, high salt does not appear to affect the binding/opening equilibrium for the R103S mutant as the calculated $K_{d,app}$ of 5.0 ± 1.2 nM is about the same as in 50 mM NaCl. The average $K_{d,app}$ value for β-S109C/Q299C-$(AF488)_2$ is modestly lower in 500 mM NaCl ($K_{d,app}$ = 5.3 ± 2.4 nM) than in 50 mM NaCl ($K_{d,app}$ = 7.0 ± 0.4 nM), but the difference is within experimental error. Together, these experiments show that the R103S mutation and high salt concentrations have only a modest effect on clamp loader–clamp binding/opening equilibria. This result is in contrast to the β monomer–dimer equilibrium where the R103S mutation and high salt dramatically shift the equilibrium toward the monomer (Purohit *et al.*, *Biophysical Journal* (2017)).

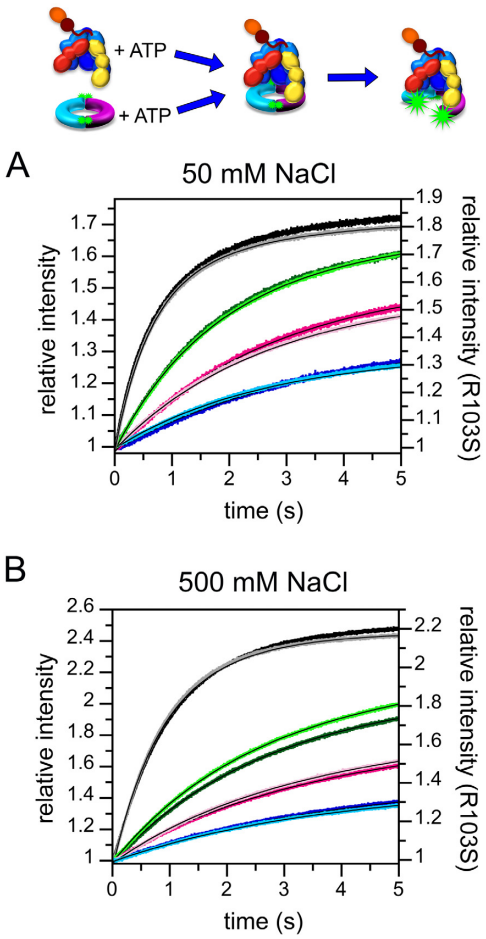

Figure 3. Clamp loader–clamp binding/opening reactions at 20°C. The increase in AF488 fluorescence that occurs when γ_{cx} binds β-$(AF488)_2$ to form an open complex was measured as a function of time when a solution of γ_{cx} and ATP (0.5 mM) in stopped-flow assay buffer was added to a solution of β-S109C/Q299C-$(AF488)_2$ (dark colors) or β-S109C/Q299C/R103S-$(AF488)_2$ (light colors) and ATP (0.5 mM) in stopped-flow assay buffer. The concentration of γ_{cx} was varied and the concentration of β was held constant at 20 nM. Representative reactions are shown that contain 10 nM (blue), 20 nM (magenta), 40 nM (green) or 160 nM (black/grey) γ_{cx} and (**A**) 50 mM NaCl or (**B**) 500 mM NaCl

Dimer interface destabilization does not increase rates of clamp opening reactions

The equilibrium clamp opening reaction consists of at least two steps, clamp binding and clamp opening (36,38). It is possible that destabilization of the β-dimer interface promotes the clamp opening step, but that a compensatory change in another step reduces the effects of destabilization on the overall binding/opening equilibrium. To test this possibility, pre-steady-state rates of clamp opening were measured to determine whether the R103S mutation or 500 mM NaCl promote the clamp opening step. Clamp opening reactions were initiated by mixing a solution of γ_{cx} and ATP with a solution of β-S109C/Q299C-$(AF488)_2$ or β-S109C/Q299C/R103S-$(AF488)_2$ and ATP. The concentration of γ_{cx} was varied from 0.005 to 1.6 μM (representative reaction time courses are shown in Figure 3A), and the concentration of β-S109C/Q299C-$(AF488)_2$ or β-S109C/Q299C/R103S-$(AF488)_2$ was held constant. The increase in AF488 fluorescence that occurs when clamps are opened was measured as a function of time in assay buffer containing 50 mM NaCl. The magnitude of increase in fluorescence differs for the two clamps because the labeling efficiency differs, but surprisingly, the time-dependent changes in fluorescence due to opening β-S109C/Q299C-$(AF488)_2$ and β-S109C/Q299C/R103S-$(AF488)_2$ are the same within experimental error. Even though the R103S mutation increases the rate of β dimer dissociation into monomers, this destabilization of the dimer interface does not increase the rate of ring opening by γ_{cx}. The clamp opening experiment was repeated in assay buffer containing 500 mM NaCl. Again, time courses for clamp opening for β-S109C/Q299C-$(AF488)_2$ and for β-S109C/Q299C/R103S-$(AF488)_2$ were similar to each other (Figure 3B) in contrast to the marked instability of the β-R103S mutant at high salt concentrations (Purohit *et al.*, *Biophysical Journal* (2017)). If clamp opening were dependent on stability of the interface, opening for the R103S mutant should have been faster. If the higher salt concentration were promoting clamp opening, rates for opening both clamps should have been faster in 500 mM NaCl than in 50 mM NaCl, but at the

higher salt concentration, the overall rate of opening was about 2-fold slower. This reduction in rates may be due to effects of increased salt concentration on interactions other than at the dimer interface such as clamp loader–clamp binding or ATP binding. Nonetheless, these kinetic experiments demonstrate clamp opening by the clamp loader is not dependent on clamp stability.

Dimer interface destabilization modestly increases lifetimes of clamp loader●clamp complexes

Because the overall association rates of γ_{cx} with β-S109C/Q299C-$(AF488)_2$ and β-S109C/Q299C/R103S-$(AF488)_2$ are the same, but $K_{d,app}$ values differ, albeit modestly, the difference in $K_{d,app}$ values should be reflected in differences in dissociation rates. Dissociation of clamps from clamp loader–clamp complexes was measured to test this and to determine whether the R103S mutation or 500 mM NaCl affect the lifetime of clamp loader–clamp complexes. In these experiments, a solution of γ_{cx}, β-$(AF488)_2$ (20 nM final), and ATP (0.5 mM) was added to a solution of unlabeled β (400 nM final) and ATP (0.5 mM). The excess unlabeled β traps clamp loaders that dissociate from AF488-labeled clamps to permit measurement of the decrease in fluorescence that occurs when γ_{cx} dissociates from β-$(AF488)_2$ and the ring closes. In reactions with 50 mM NaCl, the overall rate of dissociation of β-S109C/Q299C-$(AF488)_2$ is about twice that of β-S109C/Q299C/R103S-$(AF488)_2$ (Figure 4A). In other words, the R103S mutation that destabilizes the β-dimer interface increases the lifetime of a clamp loader–clamp complex. Time courses for dissociation of both clamps were biphasic (Table 2) indicating that dissociation occurs from two different states at different rates. In reactions with 500 mM NaCl, the overall rate of dissociation for β-S109C/Q299C-$(AF488)_2$ decreased modestly, and the dissociation rate for β-S109C/Q299C/R103S-$(AF488)_2$ increased modestly, such that the difference in overall dissociation rates for the two clamps was smaller as were the differences in $K_{d,app}$ values (Figure 4B). Decreases in fluorescence were also biphasic for both clamps in 500 mM NaCl. In general, the differences dissociation rates can account for the differences in equilibrium dissociation constants.

The R103S mutation does not affect rates of clamp closing on DNA

In addition to forming stable open clamp complexes, clamp loaders also chaperone clamps to DNA where the clamps are deposited and closed to encircle DNA (recently reviewed in (10,12)). It is possible that destabilization of the β-dimer interface affects the rate at which clamps reform a closed dimer interface. To test this possibility, clamp closing on DNA was measured for β-S109C/Q299C-$(AF488)_2$ and β-S109C/Q299C/R103S-$(AF488)_2$. This experiment used a symmetrical DNA substrate with two ss/ds DNA junctions of the same polarity with 5′-ssDNA overhangs (39). Single-stranded binding protein (SSB) was included in reactions because ssDNA is bound by SSB *in vivo* (27,28). Clamp loading reactions, in buffer with 50 mM NaCl,

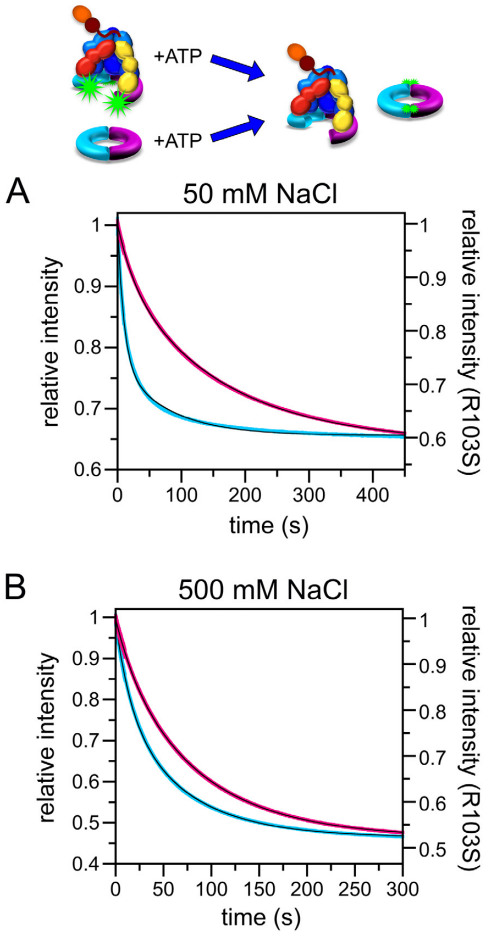

Figure 4. Clamp loader–clamp dissociation reactions at 20°C. The decrease in fluorescence that occurs when β-$(AF488)_2$ dissociates from γ_{cx} was measured in assays containing 40 nM γ_{cx}, 10 nM β-S109C/Q299C-$(AF488)_2$ (cyan) or β-S109C/Q299C/R103S-$(AF488)_2$ (magenta), 400 nM unlabeled β, and 0.5 mM ATP in buffer with (**A**) 50 mM NaCl or (**B**) 500 mM NaCl. Data were fit to the sum of two exponentials (black lines through traces), and rate constants and fractional amplitudes derived from fits are given in Table 2.

were initiated by adding a solution of γ_{cx}, β-$(AF488)_2$, and ATP to a solution of DNA, SSB, excess unlabeled β-clamp, and ATP. Excess unlabeled clamp is added to limit the reaction to a single observable cycle of clamp closing. When the clamp closes around DNA, AF488 fluorescence is quenched. The rates of β-S109C/Q299C-$(AF488)_2$ and β-S109C/Q299C/R103S-$(AF488)_2$ closing on DNA are similar differing by no more than is typical of experimental variation (Figure 5). These results along with those measuring clamp opening rates (Figure 3) show that the R103S mutation that destabilizes the β-dimer interface has little if any effect on the clamp loading reaction either at the clamp opening step where a dimer interface is broken or at the clamp closing step where a dimer interface reforms.

Effects of γ complex binding on the fluorescence of singly-labeled β-clamps

To further define the clamp opening step of the clamp loading reaction, kinetic data were modeled to define individual

Table 2. Clamp loader–clamp dissociation rate constants and amplitudes

	50 mM NaCl				500 mM NaCl			
	a_f[a]	k_f (s^{-1})[b]	a_s	k_s (s^{-1})	a_f	k_f (s^{-1})	a_s	k_s (s^{-1})
β-S109C/Q299C-$(AF488)_2$	0.66	0.10	0.34	0.013	0.38	0.064	0.62	0.015
β-S109C/Q299C R103S-$(AF488)_2$	0.23	0.039	0.77	0.0098	0.18	0.046	0.82	0.012
β−R103S/I305C−$(AF488)_2$	0.28	0.058	0.72	0.011				

[a]a_f and a_s are fractional amplitudes for fast and slow phases, respectively.
[b]k_f and k_s are rate constants for fast and slow phases, respectively.

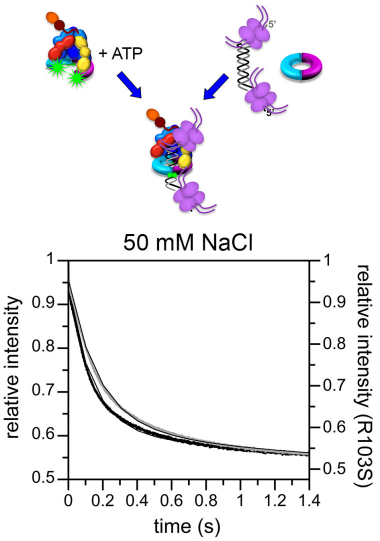

Figure 5. Clamp loading on DNA bound by SSB at 20°C. The decrease in AF488 fluorescence that occurs when clamps are closed on DNA was measured in stopped-flow reactions in which a solution of γ_{cx}, β-$(AF488)_2$, and ATP were mixed with a solution of SSB-bound DNA and excess unlabeled β. DNA is symmetrical, as illustrated, with two 30-nt single-stranded 5′ DNA overhangs and a 30-nt duplex. Final concentrations were 20 nM β-S109C/Q299C-$(AF488)_2$ or β-S109C/Q299C/R103S-$(AF488)_2$, 20nM γ_{cx}, 200 nM unlabeled β, 160 nM DNA, 960 nM SSB and 0.5 mM ATP in stopped-flow assay buffer containing 50 mM NaCl.

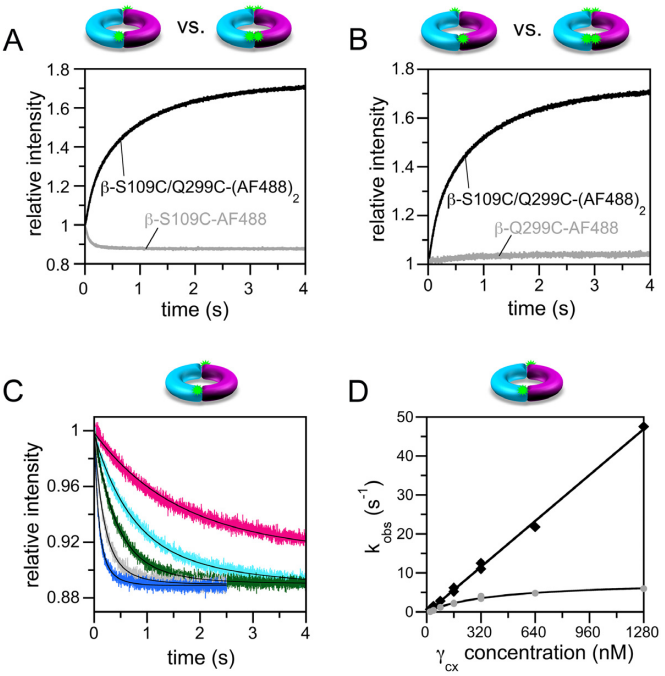

Figure 6. Clamp loader binding to singly AF488-labeled clamps affects AF488 fluorescence. Binding reactions were measured side-by-side in stopped-flow experiments for β-S109C/Q299C-$(AF488)_2$, β-S109C-AF488, and β-Q299C-AF488. Fluorescence intensity is plotted relative to the signal for unbound clamp in each case, but note the absolute fluorescence for singly-labeled clamps is greater than for the doubly-labeled clamp because there is no AF488-dimer quenching. (**A**) Clamp binding for β-S109C/Q299C-$(AF488)_2$ (black) versus β-S109C-AF488 (grey) is shown. (**B**) Clamp binding for β-S109C/Q299C-$(AF488)_2$ (black) versus β-Q299C-AF488 (grey) is shown. (**C**) Rates of γ_{cx} binding to β-S109C-AF488 were measured in reactions containing 20 nM β-S109C-AF488, 0.5 mM ATP, and 20 (magenta), 40 (light blue), 80 (green), 160 (grey) and 320 (dark blue) nM γ_{cx} in stopped-flow assay buffer containing 50 mM NaCl. (**D**) Time courses from panel C were fit to double exponentials, and observed rate constants for the rapid (black diamonds) and slow (grey circles) phases obtained from the fits are plotted as a function of γ_{cx} concentration.

kinetic steps. As a control prior to kinetic modeling, singly-labeled clamps were made to determine whether AF488 fluorescence in β-S109C/Q299C-$(AF488)_2$ could be affected by mechanisms other than the unstacking of AF488 dimers that occurs on clamp opening. Clamp binding/opening reactions were measured for singly AF488-labeled clamps that contained either the S109C mutation or Q299C mutation. The fluorescence of AF488 changed when both singly-labeled clamps were bound by γ_{cx}, but the changes were different. There was a *rapid decrease* in AF488 fluorescence when β-S109C-AF488 was bound by γ_{cx} (Figure 6A) and a *slower increase* in fluorescence when β-Q299C-AF488 was bound by γ_{cx} (Figure 6B). Because these fluorophores are located on the surface of β (Figure 1), at or near sites where γ_{cx} contacts the clamp, these changes are likely due to environmental effects of fluorophore interactions with γ_{cx}. The rapid decrease in fluorescence for β-S109C-AF488 reflects the binding of γ_{cx} to β because the rate of change is faster than clamp opening as measured previously (36), and the time course is a simple exponential function. The small increase in AF488 fluorescence that occurs when γ_{cx} binds β-Q299C-AF488 is on the same time scale as clamp opening, and most likely results from conformational changes that occur on opening and affect the environment of the fluorophore possibly by increasing interactions with γ_{cx} (e.g. as in Figure 1). The environmental changes in AF488 fluorescence for the single mutants must also occur in the doubly-labeled clamps containing both S109C and Q299C mutations. This means that fluorescence changes for the β-S109C/Q299C mutants are a composite of environmental changes due to interactions with the clamp loader and

destacking of the fluorophores due to clamp opening. The overlapping changes in fluorescence complicate the analyses of time-dependent changes in fluorescence during clamp opening reactions, and data cannot be modeled to a simple two-state system with a low quantum yield for closed clamps and a high quantum yield for open clamps.

Kinetic modeling of γ complex binding and opening β

To simplify the system for kinetic modeling, clamp opening kinetics were measured for a doubly-labeled clamp where the fluorophores are located on the face of β that is not bound by γ_{cx} (Figure 1). Arg-103 and Ile-305 were mutated to Cys and labeled with AF488 (β-R103C/I305C-$(AF488)_2$). Note that this clamp contains a destabilizing Arg-103 mutation and could not be used for experiments where opening of clamps with and without an Arg mutation was measured. Fluorescence of AF488 in both single mutants, β-R103C-AF488 and β-I305C-AF488, is not affected by clamp loader binding (36). This is further supported by measurements of fluorescence lifetimes for doubly-labeled β-R103C/I305C-$(TMR)_2$ which show that γ_{cx} binding does not affect the fluorescence lifetimes. Clamp loader binding decreases the amplitude of the short lifetime term (quenched state) associated with the closed clamp and increases the amplitude of the long lifetime term (unquenched state) associated with the open clamp (Supplementary Figure S3). These lifetime measurements utilized TMR rather than AF488 because the excitation wavelength of TMR was better matched to the laser system used for the measurements. Both these lifetime measurements with the doubly-labeled β-R103C/I305C-$(TMR)_2$ clamp and previous steady-state fluorescence measurements with the singly-AF488-labeled clamps support the assumption that changes in fluorescence are due to changes in stacking interactions between the two fluorophores that occur when the clamp opens and closes with no contributions from environmental changes due to protein interactions. Therefore, we assume that there are only two fluorescence states for β-R103C/I305C-$(AF488)_2$, one for the open clamp where a pair of fluorophores is unstacked and unquenched, and one for the closed clamp where fluorophores are stacked and quenched. Because the fluorescence of AF488 covalently bound to β-R103C/I305C-$(AF488)_2$ is not affected by interactions with the clamp loader, the time course for binding/opening reactions differ in shape from those for β-S109C/Q299C-$(AF488)_2$ (Supplementary Figure S4).

Given that AF488 fluorescence for the single β-S109C-AF488 mutant is sensitive to clamp loader binding, this mutant was used to measure rates of γ_{cx} binding to the β-clamp. Two data sets for reactions containing 50 mM NaCl were used for kinetic modeling: (i) γ_{cx} binding to β-S109C-AF488 (Figure 6C) and (ii) γ_{cx}-catalyzed opening of β-R103C/I305C-$(AF488)_2$ (Supplementary Figure S5). Clamp binding was measured in reactions containing 10–1280 nM γ_{cx} and 20 nM β-S109C-AF488, and clamp opening was measured in reaction containing 5–1800 nM γ_{cx} and 16 nM β-R103C/I305C-$(AF488)_2$. As a starting point, these data were empirically fit to sums of exponentials. Data for γ_{cx} binding β-S109C-AF488 are best fit by a double exponential. Calculated rate constants for the rapid phase are a linear function of γ_{cx} concentration as expected for a *binding* reaction (Figure 6D, black diamonds). The slope yields an apparent second order rate constant of 3.7×10^7 M^{-1} s^{-1} which is consistent with our previous measurements (2.3×10^7 M^{-1} s^{-1}) using another assay (40). Rate constants for the slower phase approach a maximum value of 8 s^{-1} consistent with the slow phase reflecting the clamp opening step. When data for γ_{cx} opening β-R103C/I305C-$(AF488)_2$ are fit by a double exponential, the calculated rate constants are not a linear function of γ_{cx} but curve approaching limiting values of 11 s^{-1} for the rapid phase and 1.5 s^{-1} for the slow phase (Supplementary Figure S5). This is comparable to our previous studies where maximal rates were 9 and 0.8 s^{-1} for the fast and slow phases, respectively (36). Note that time courses for opening reactions are not simple exponentials and contain a short lag phase, but exponential fits were used to estimate rates of change in fluorescence. Both the shape of the opening time course and the change in rate constant with γ_{cx} concentration are consistent with a mechanism that contains at least two-steps, binding then opening (36). Dissociation of β-R103C/I305C-$(AF488)_2$ from a clamp loader–clamp complex is biphasic and occurs at a rate similar to that for β-S109C/Q288C/R103S-$(AF488)_2$ (Supplementary Figure S5 and Table 2).

Empirical analysis of kinetic data above indicates that the clamp opening reaction is at least a two-step reaction consisting of an initial clamp loader–clamp binding step followed by a clamp opening step (36,38). However, global fitting of the β-S109C-AF488 and β-R103C/I305C-$(AF488)_2$ binding/opening reactions to this simple kinetic model does not adequately fit the data (Supplementary Figure S6). The complexity of the kinetic model was increased by including an additional open state which is consistent with the biphasic change in fluorescence in clamp opening reactions. Clamp binding reactions using β-S109C-AF488 and clamp opening reactions using β-R103C/I305C-$(AF488)_2$ were globally fit to a kinetic model in which the clamp loader binds the clamp to form a closed clamp loader–clamp complex, the clamp opens relatively rapidly, and there is a conformational rearrangement in the open clamp loader–clamp complex that stabilizes the open state (Figure 7). This three-step model fits the data better than the two-step model. We note that these kinetic data could also be fit to a model that includes two parallel two-step binding-opening reactions in which a fraction of the total β is bound and open faster than the rest. This parallel model does not make intuitive sense because it requires that two separate populations of β exist and react at different rates. We favor the first model based on structural data as explained in the Discussion.

DISCUSSION

Although many mechanistic questions about the clamp loading reaction mechanism have been answered, questions regarding the mechanism of clamp opening remain. Does the clamp loader depend on intrinsic clamp opening and closing dynamics to form an open clamp loader–clamp complex? Or does the clamp loader destabilize and actively open clamps? What are the steps in the clamp opening reaction? Clamp opening reactions catalyzed by the *E. coli* and

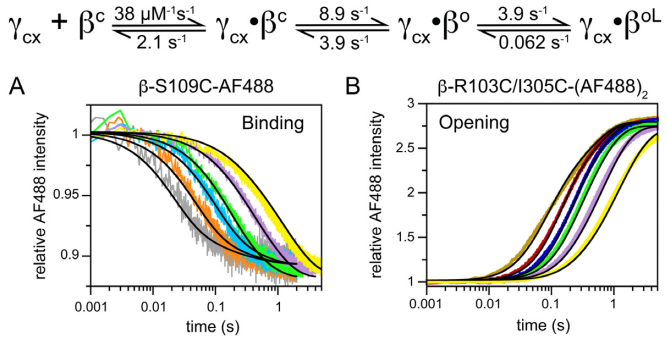

Figure 7. Clamp loader binding to β-S109C-AF488 and opening β-R103C/Q299C-$(AF488)_2$ were fit to the model shown in the scheme where γ complex (γ_{cx}) binds a closed β-clamp (β^c) to form a closed complex, the clamp opens (β^o) to form an open complex, and conformational rearrangements occur to form a 'locked open' clamp (β^{oL}). (**A**) Clamp binding reactions containing 40 (yellow), 80 (lavender), and 160 nM (green), 320 (light blue), 640 (orange) and 1280 nM (grey) γ_{cx} are shown. (**B**) Clamp opening reactions containing 40 (yellow), 80 (lavender), 160 nM (green), 250 nM (blue), 500 nM (red) and 1800 nM (tan) γ_{cx} are shown. Black lines through the data are the result of the fit of the model using KinTek Explorer with rate constants shown in the scheme.

S. cerevisiae clamp loaders are at least two-step reactions consisting of an initial binding step followed by an opening step (36,38,41). But, a two-step binding-opening mechanism does not necessarily mean that the clamp loaders actively open clamps; the clamp loaders could bind closed clamps, which predominate in solution, and 'wait' for the clamps to open spontaneously. To address these outstanding questions, the mechanism of the clamp opening reaction was investigated.

Conditions that destabilize the dimer interface of the β-clamp and promote dissociation into monomers have been identified (Purohit *et al.*, *Biophysical Journal* (2017)). Electrostatic interactions between positively charged residues on one side of the dimer interface (N-terminal protein domain) and negatively charged residues on the other (C-terminal domain) can be disrupted by high NaCl concentrations to promote dissociation into monomers (42). Additionally, a point mutation converting a positively charged Arg residue to a neutral amino acid residue destabilizes the dimeric form of the clamp. This manuscript uses these conditions that destabilize the β-dimer interface to determine whether the clamp loading reaction, and in particular, the clamp opening step is dependent on the stability and dynamics of the β dimer interface. Mutation of Arg-103 substantially destabilizes the dimer interface decreasing the lifetime of the dimeric form of the clamp from 34 to 5.8 h, and similarly, increasing the NaCl concentration from 50 to 500 mM reduces the lifetime to 9 h (Purohit *et al.*, *Biophysical Journal* (2017)). The combination of the Arg-103 mutation and high salt leads to even greater destabilization such that the majority of clamps dissociate into monomers within the 20 min it takes to measure the populations of monomers and dimers (Purohit *et al.*, *Biophysical Journal* (2017)). Although these conditions substantially destabilize the β-dimer interface, mutation of Arg-103 to Ser does not affect the rate of clamp opening either at a low salt concentration (50 mM NaCl, Figure 3A), or a high salt concentration (500 mM NaCl, Figure 3B). If the clamp opening reaction were dependent on the dynamics and the stability of the β-clamp, the R103S mutation would be expected to increase the rate of clamp opening because the mutation destabilizes the interface. Furthermore, there is no evidence that spontaneous clamp opening events are frequent enough to support clamp loading (Purohit *et al.*, *Biophysical Journal* (2017)). Destabilizing the clamp interface might also be expected to affect the ease with which the clamp closes, but the R103S mutation did not affect rates of clamp closing on DNA either. Given that destabilization of the β-dimer interface does not promote clamp opening, it is unlikely that the clamp loader binds the β-clamp and depends on spontaneous opening events to form an open clamp loader–clamp complex. Instead, these results are consistent with a mechanism in which the clamp loader destabilizes and actively opens the clamp.

The clamp opening mechanism was investigated further by measuring the kinetics of the clamp loader–clamp binding (β-S109C-AF488) and opening (β-R103C/I305C-$(AF488)_2$) to define a kinetic mechanism for the reaction. Previous work and empirical fitting of the current data show that the clamp opening reaction is at least a two-step binding-opening reaction (36,38,41), however, this simple model did not adequately fit clamp opening kinetic data (Supplementary Figure S6). In addition, the biphasic nature of clamp opening kinetics indicate that there are two open states. Therefore, kinetic data for clamp binding and clamp opening were fit to a three-step 'bind-open-lock' model in which the clamp loader binds a closed clamp, the clamp opens, and the initial open clamp loader–clamp complex undergoes a conformational rearrangement that 'locks' the complex in an open state (Figure 7). This simple bind-open-lock model fits the data reasonably well, but the reaction likely contains additional kinetic steps. For example, in the bind-open-lock model, the clamp only dissociates from the closed clamp loader–clamp complex, but there are likely other pathways for dissociation such as from open complexes or following ATP hydrolysis. Clamp loader–clamp dissociation kinetics are biphasic, and the rate of the slow phase is the same for all clamps under all conditions, ~0.01 s^{-1} (Table 2). It is interesting to note that this rate is the same as the slow ATP hydrolysis (k_{cat} = 0.012 s^{-1}) that occurs in the clamp loader–clamp complex in the absence of DNA (21). We speculate that β may dissociate from the 'locked open' complex at a rate that is limited by this slow rate of ATP hydrolysis. There is not enough information in the kinetic data to add or rule out this or other kinetic steps. However, any missing steps are not likely affecting rates or populations of species to a large extent because the minimal bind-open-lock model recapitulates the key features of the kinetic data.

In the bind-open-lock model, the initial clamp opening step does not strongly favor an open conformation of the clamp; the open clamp loader–clamp complex is favored over the closed complex by about 2-to-1 (Figure 7). It is the subsequent conformational change step strongly favors the open state with a forward rate that is ~60-fold greater than the reverse rate. The bind-open-lock model can be envisioned in terms of structural data for clamp loader–clamp complexes. When the clamp loader initially binds the closed

clamp, the most extensive interactions are likely to be between the δ subunit (Figure 1, yellow) and the β-clamp (43). Interactions between the other clamp loader subunits and the clamp are likely to be less extensive or nonexistent as in the *S. cerevisiae* closed clamp loader–clamp complex (Figure 1) (44). The yeast clamp loader–clamp complex was trapped in a closed state by mutations to conserved 'Arg finger' residues, and these mutations shift the opening-closing equilibrium to favor the closed state in solution (45,46). Initial opening of the clamp may not substantially increase contacts between the clamp loader and the clamp, and therefore, the clamp readily closes. Subsequent conformational rearrangements in the open clamp loader–clamp complex may be required to form a locked open state where *all five* of the core clamp loader subunits interact extensively with the face of the clamp as in the crystal structure of a bacteriophage clamp loader–clamp complex (Figure 1) and the EM structures of an archaeal clamp loader–clamp complex (29,30). The extensive contacts between the clamp loader and clamp may not only stabilize the open state, but also prevent dimeric or trimeric clamps from dissociating into monomers when the rings are open. Oligomer association is highly cooperative for trimeric clamps suggesting that opening one interface would destabilize clamps and favor dissociation into monomers (13,32,47). The free energy of binding for two or three identical interfaces contributes to the stability of sliding clamps, and if one of these interaction surfaces is lost as it is on clamp opening, this would substantially destabilize the oligomeric form. By engaging the clamp with all five clamp loader subunits, open clamps can be stabilized by the clamp loader to prevent dissociation into monomers before the clamp is loaded onto DNA.

The proposal that clamp loaders actively open clamps that exist predominantly as closed rings in solution was initially made based on the high stability of the closed ring forms of these clamps (31). The structure the δ subunit of the *E. coli* clamp loader bound to a β monomer suggested that that the δ subunit distorts and destabilizes the β-dimer interface which causes the clamp to open supporting an active role for the clamp loader in clamp opening (43). Results from this work support a mechanism where the *E. coli* clamp loader actively opens the β-clamp rather than capturing clamps that have spontaneously opened. The bind-open-lock model predicts that clamp opening and closing dynamics ($k_{open} = 9\ s^{-1}$ and $k_{close} = 4\ s^{-1}$) occur on a time scale that could be detected by fluorescence correlation spectroscopy if the unbound clamp had similar dynamics and occurred at a reasonable frequency, however, this was not the case (Purohit *et al.*, *Biophysical Journal* (2017)). Therefore, we conclude that the clamp loader alters these dynamics. Active β-clamp opening does not contradict results from hydrogen–deuterium exchange studies showing that the β-dimer interface is dynamic because minor fluctuations in the backbone conformation could allow for hydrogen–deuterium exchange, and because exchange takes place on a long time scale (≈3.5 h) suggesting that opening events are infrequent (34). Nor does an active clamp opening model imply that the clamp loader only destabilizes the clamp to promote opening. The bind-open-lock model suggests that a conformational change occurs the after initial clamp opening event to strongly stabilize an open clamp loader–clamp conformation (locked open complex). The insensitivity of clamp opening rates to destabilization of the β-dimer interface and the bind-open-lock model show that the clamp loader both destabilizes the closed clamp and stabilizes the open clamp. This finding differs somewhat from molecular dynamics simulations suggesting that the clamp loader does not substantially destabilize the closed clamp, but instead stabilizes the open clamp (33). This difference may simply be due to the differences in the clamp loader–clamps used in the two studies. The molecular dynamics simulations were based on interactions between the eukaryotic clamp loader and trimeric PCNA clamp, and it may be that the eukaryotic clamp loader does not actively open the clamp. The PCNA clamp is less stable than the β-clamp; PCNA dissociates from circular DNA molecules about 3-times faster than β at 37°C and the lifetime of the PCNA trimer is ∼10-fold shorter than the lifetime of the β dimer at 20°C (31,32). This decreased stability of PCNA may lead to more frequent spontaneous opening events and allow the eukaryotic clamp loader to capture open PCNA clamps passively. On the other hand, the molecular dynamics simulations were based on structural data for the Arg finger mutant which is defective in clamp opening, and thus, may not be not be giving the complete picture (Figure 1) (44–46). Although PCNA is not as stable as the β-clamp, the lifetime of the trimeric PCNA ring (4.5 h) is about the same as the lifetime of the β-R103S mutant (5.8 h) at room temperature which suggests that the clamp loader may also need to destabilize PCNA to form an open complex.

The results in this paper support a model in which the *E. coli* clamp loader binds a closed clamp and destabilizes the clamp to form an initial open clamp loader–clamp complex. This initial opening event does not strongly favor an open clamp loader–clamp complex, and subsequent conformational changes in the clamp loader–clamp complex are needed to stabilize the clamp in an open conformation. This final locked open state likely represents a complex where all five core clamp loader subunits interact extensively with the face of the clamp to stabilize the open conformation. Because breaking one interface in forming an open clamp would likely destabilize clamps, another important function of this final locked open complex is to prevent dissociation of open clamps into monomers.

SUPPLEMENTARY DATA

Supplementary Data are available at NAR Online.

FUNDING

National Science Foundation [MCB-1157765 to M.L. and L.B]. Funding for open access charge: University of Florida.
Conflict of interest statement. None declared.

REFERENCES

1. Wickner,W., Schekman,R., Geider,K. and Kornberg,A. (1973) A new form of DNA polymerase 3 and a copolymerase replicate a long, single-stranded primer-template. *Proc. Natl. Acad. Sci. U.S.A.*, **70**, 1764–1767.

2. Hurwitz,J. and Wickner,S. (1974) Involvement of two protein factors and ATP in *in vitro* DNA synthesis catalyzed by DNA polymerase 3 of Escherichia coli. *Proc. Natl. Acad. Sci. U.S.A.*, **71**, 6–10.
3. Piperno,J.R. and Alberts,B.M. (1978) An ATP stimulation of T4 DNA polymerase mediated via T4 gene 44/62 and 45 proteins. The requirement for ATP hydrolysis. *J. Biol. Chem.*, **253**, 5174–5179.
4. Fay,P.J., Johanson,K.O., McHenry,C.S. and Bambara,R.A. (1982) Size classes of products synthesized processively by two subassemblies of *Escherichia coli* DNA polymerase III holoenzyme. *J. Biol. Chem.*, **257**, 5692–5699.
5. Vivona,J.B. and Kelman,Z. (2003) The diverse spectrum of sliding clamp interacting proteins. *FEBS Lett.*, **546**, 167–172.
6. Maga,G. and Hübscher,U. (2003) Proliferating cell nuclear antigen (PCNA): a dancer with many partners. *J. Cell Sci.*, **116**, 3051–3060.
7. Moldovan,G.-L., Pfander,B. and Jentsch,S. (2007) PCNA, the maestro of the replication fork. *Cell*, **129**, 665–679.
8. Stukenberg,P.T., Studwell-Vaughan,P.S. and O'Donnell,M. (1991) Mechanism of the sliding beta-clamp of DNA polymerase III holoenzyme. *J. Biol. Chem.*, **266**, 11328–11334.
9. Kong,X.P., Onrust,R., O'Donnell,M. and Kuriyan,J. (1992) Three-dimensional structure of the beta subunit of *E.coli* DNA polymerase III holoenzyme: a sliding DNA clamp. *Cell*, **69**, 425–437.
10. Hedglin,M., Kumar,R. and Benkovic,S.J. (2013) Replication Clamps and Clamp Loaders. *Cold Spring Harb. Perspect. Biol.*, **5**, a010165.
11. Georgescu,R., Langston,L. and O'Donnell,M. (2015) A proposal: Evolution of PCNA's role as a marker of newly replicated DNA. *DNA Repair (Amst.)*, **29**, 4–15.
12. Kelch,B.A. (2016) Review: the lord of the rings: structure and mechanism of the sliding clamp loader. *Biopolymers*, **105**, 532–546.
13. Alley,S.C., Shier,V.K., Abel-Santos,E., Sexton,D.J., Soumillion,P. and Benkovic,S.J. (1999) Sliding clamp of the bacteriophage T4 polymerase has open and closed subunit interfaces in solution. *Biochemistry*, **38**, 7696–7709.
14. Alley,S.C., Abel-Santos,E. and Benkovic,S.J. (2000) Tracking sliding clamp opening and closing during bacteriophage T4 DNA polymerase holoenzyme assembly. *Biochemistry*, **39**, 3076–3090.
15. Liu,C., McKinney,M.C., Chen,Y.-H., Earnest,T.M., Shi,X., Lin,L.-J., Ishino,Y., Dahmen,K., Cann,I.K.O. and Ha,T. (2011) Reverse-chaperoning activity of an AAA+ protein. *Biophys. J.*, **100**, 1344–1352.
16. Koonin,E.V. (1993) A superfamily of ATPases with diverse functions containing either classical or deviant ATP-binding motif. *J. Mol. Biol.*, **229**, 1165–1174.
17. Davey,M.J., Jeruzalmi,D., Kuriyan,J. and O'Donnell,M. (2002) Motors and switches: AAA+ machines within the replisome. *Nat. Rev. Mol. Cell Biol.*, **3**, 826–835.
18. Erzberger,J.P. and Berger,J.M. (2006) Evolutionary relationships and structural mechanisms of AAA+ proteins. *Annu. Rev. Biophys. Biomol. Struct.*, **35**, 93–114.
19. Berdis,A.J. and Benkovic,S.J. (1996) Role of adenosine 5′-triphosphate hydrolysis in the assembly of the bacteriophage T4 DNA replication holoenzyme complex. *Biochemistry*, **35**, 9253–9265.
20. Turner,J., Hingorani,M.M., Kelman,Z. and O'Donnell,M. (1999) The internal workings of a DNA polymerase clamp-loading machine. *EMBO J.*, **18**, 771–783.
21. Hingorani,M.M., Bloom,L.B., Goodman,M.F. and O'Donnell,M. (1999) Division of labor–sequential ATP hydrolysis drives assembly of a DNA polymerase sliding clamp around DNA. *EMBO J.*, **18**, 5131–5144.
22. Bertram,J.G., Bloom,L.B., Hingorani,M.M., Beechem,J.M., O'Donnell,M. and Goodman,M.F. (2000) Molecular mechanism and energetics of clamp assembly in *Escherichia coli*. The role of ATP hydrolysis when gamma complex loads beta on DNA. *J. Biol. Chem.*, **275**, 28413–28420.
23. Gomes,X.V. and Burgers,P.M. (2001) ATP utilization by yeast replication factor C. I. ATP-mediated interaction with DNA and with proliferating cell nuclear antigen. *J. Biol. Chem.*, **276**, 34768–34775.
24. Gomes,X.V., Schmidt,S.L. and Burgers,P.M. (2001) ATP utilization by yeast replication factor C. II. Multiple stepwise ATP binding events are required to load proliferating cell nuclear antigen onto primed DNA. *J. Biol. Chem.*, **276**, 34776–34783.
25. Fotedar,R., Mossi,R., Fitzgerald,P., Rousselle,T., Maga,G., Brickner,H., Messier,H., Kasibhatla,S., Hübscher,U. and Fotedar,A. (1996) A conserved domain of the large subunit of replication factor C binds PCNA and acts like a dominant negative inhibitor of DNA replication in mammalian cells. *EMBO J.*, **15**, 4423–4433.
26. Uhlmann,F., Cai,J., Gibbs,E., O'Donnell,M. and Hurwitz,J. (1997) Deletion analysis of the large subunit p140 in human replication factor C reveals regions required for complex formation and replication activities. *J. Biol. Chem.*, **272**, 10058–10064.
27. Glover,B.P. and McHenry,C.S. (1998) The chi psi subunits of DNA polymerase III holoenzyme bind to single-stranded DNA-binding protein (SSB) and facilitate replication of an SSB-coated template. *J. Biol. Chem.*, **273**, 23476–23484.
28. Kelman,Z., Yuzhakov,A., Andjelkovic,J. and O'Donnell,M. (1998) Devoted to the lagging strand-the subunit of DNA polymerase III holoenzyme contacts SSB to promote processive elongation and sliding clamp assembly. *EMBO J.*, **17**, 2436–2449.
29. Miyata,T., Suzuki,H., Oyama,T., Mayanagi,K., Ishino,Y. and Morikawa,K. (2005) Open clamp structure in the clamp-loading complex visualized by electron microscopic image analysis. *Proc. Natl. Acad. Sci. U.S.A.*, **102**, 13795–13800.
30. Kelch,B.A., Makino,D.L., O'Donnell,M. and Kuriyan,J. (2011) How a DNA polymerase clamp loader opens a sliding clamp. *Science*, **334**, 1675–1680.
31. Yao,N., Turner,J., Kelman,Z., Stukenberg,P.T., Dean,F., Shechter,D., Pan,Z.Q., Hurwitz,J. and O'Donnell,M. (1996) Clamp loading, unloading and intrinsic stability of the PCNA, beta and gp45 sliding clamps of human, *E. coli* and T4 replicases. *Genes Cells*, **1**, 101–113.
32. Binder,J.K., Douma,L.G., Ranjit,S., Kanno,D.M., Chakraborty,M., Bloom,L.B. and Levitus,M. (2014) Intrinsic stability and oligomerization dynamics of DNA processivity clamps. *Nucleic Acids Res.*, **42**, 6476–6486.
33. Tainer,J.A., McCammon,J.A. and Ivanov,I. (2010) Recognition of the ring-opened state of proliferating cell nuclear antigen by replication factor C promotes eukaryotic clamp-loading. *J. Am. Chem. Soc.*, **132**, 7372–7378.
34. Fang,J., Engen,J.R. and Beuning,P.J. (2011) *Escherichia coli* processivity clamp β from DNA polymerase III Is dynamic in solution. *Biochemistry*, **50**, 5958–5968.
35. Johnson,K.A., Simpson,Z.B. and Blom,T. (2009) Global kinetic explorer: a new computer program for dynamic simulation and fitting of kinetic data. *Anal. Biochem.*, **387**, 20–29.
36. Paschall,C.O., Thompson,J.A., Marzahn,M.R., Chiraniya,A., Hayner,J.N., O'Donnell,M., Robbins,A.H., McKenna,R. and Bloom,L.B. (2011) The *Escherichia coli* clamp loader can actively pry open the β-sliding clamp. *J. Biol. Chem.*, **286**, 42704–42714.
37. Hingorani,M.M. and O'Donnell,M. (1998) ATP binding to the *Escherichia coli* clamp loader powers opening of the ring-shaped clamp of DNA polymerase III holoenzyme. *J. Biol. Chem.*, **273**, 24550–24563.
38. Zhuang,Z., Yoder,B.L., Burgers,P.M.J. and Benkovic,S.J. (2006) The structure of a ring-opened proliferating cell nuclear antigen-replication factor C complex revealed by fluorescence energy transfer. *Proc. Natl. Acad. Sci. U.S.A.*, **103**, 2546–2551.
39. Hayner,J.N., Douma,L.G. and Bloom,L.B. (2014) The interplay of primer-template DNA phosphorylation status and single-stranded DNA binding proteins in directing clamp loaders to the appropriate polarity of DNA. *Nucleic Acids Res.*, **42**, 10655–10667.
40. Thompson,J.A., Paschall,C.O., O'Donnell,M. and Bloom,L.B. (2009) A slow ATP-induced conformational change limits the rate of DNA binding but not the rate of beta clamp binding by the *Escherichia coli* gamma complex clamp loader. *J. Biol. Chem.*, **284**, 32147–32157.
41. Thompson,J.A., Marzahn,M.R., O'Donnell,M. and Bloom,L.B. (2012) Replication factor C is a more effective proliferating cell nuclear antigen (PCNA) opener than the checkpoint clamp loader, Rad24-RFC. *J. Biol. Chem.*, **287**, 2203–2209.
42. Jergic,S., Horan,N.P., Elshenawy,M.M., Mason,C.E., Urathamakul,T., Ozawa,K., Robinson,A., Goudsmits,J.M., Wang,Y., Pan,X. *et al.* (2013) A direct proofreader-clamp interaction stabilizes the Pol III replicase in polymerization mode. *EMBO J*, **32**, 1322–1333.
43. Jeruzalmi,D., Yurieva,O., Zhao,Y., Young,M., Stewart,J., Hingorani,M., O'Donnell,M. and Kuriyan,J. (2001) Mechanism of processivity clamp opening by the delta subunit wrench of the clamp loader complex of *E. coli* DNA polymerase III. *Cell*, **106**, 417–428.

44. Bowman,G.D., O'Donnell,M. and Kuriyan,J. (2004) Structural analysis of a eukaryotic sliding DNA clamp-clamp loader complex. *Nature*, **429**, 724–730.
45. Snyder,A.K., Williams,C.R., Johnson,A., O'Donnell,M. and Bloom,L.B. (2004) Mechanism of loading the *Escherichia coli* DNA polymerase III sliding clamp: II. Uncoupling the beta and DNA binding activities of the gamma complex. *J. Biol. Chem.*, **279**, 4386–4393.
46. Sakato,M., O'Donnell,M. and Hingorani,M.M. (2011) A central swivel point in the RFC clamp loader controls PCNA opening and loading on DNA. *J. Mol. Biol.*, **416**, 163–175.
47. Singh,M.I., Ganesh,B. and Jain,V. (2016) On the domains of T4 phage sliding clamp gp45: an intermolecular crosstalk governs structural stability and biological activity. *Biochim. Biophys. Acta (BBA)-Gen.*, doi:10.1016/j.bbagen.2016.08.012.
48. Simonetta,K.R., Kazmirski,S.L., Goedken,E.R., Cantor,A.J., Kelch,B.A., McNally,R., Seyedin,S.N., Makino,D.L., O'Donnell,M. and Kuriyan,J. (2009) The mechanism of ATP-dependent primer-template recognition by a clamp loader complex. *Cell*, **137**, 659–671.